Arch. Metall. Mater. **63** (2018), 2, 539-545

DOI: 10.24425/118972

IBRAHIM MUSTAPHA ALIBE*,***#, KHAMIRUL AMIN MATORI*,**#, HAJ ABDUL AZIZ SIDEK**, YAKOOB YAZID**, ELIAS SAION**, ALI MUSTAPHA ALIBE****,*****, MOHD HAFIZ MOHD ZAID**, ENGKU ABD GHAPUR ENGKU ALI*, TASIU ZANGINA**

THE INFLUENCE OF CALCINATION TEMPERATURE ON STRUCTURAL AND OPTICAL PROPERTIES OF ZnO-SiO_2 NANOCOMPOSITE BY SIMPLE THERMAL TREATMENT ROUTE

This study offers a new method to synthesize facilely willemite (Zn_2SiO_4) based phosphor at the temperature of 800 °C. The ZnO-SiO_2 nanocomposite was calcined at different temperatures between 500 and 1000 °C. The structural, morphological and optical properties of the nanocomposite obtained at various calcination temperatures were studied using different techniques. The FT-IR, XRD and the UV-vis result confirmed the formation of willemite phase. The precursor was confirmed to be amorphous by XRD at room temperature, but upon calcination temperature at 500 °C, it was transformed into a crystalline structure. The crystallinity and the particle size of the nanocomposite increase as the calcination temperature were increased as revealed by XRD and TEM measurement. The sample exhibits a spherical morphology from 500 to 800 °C and dumbbell-like morphology above 800 °C as shown by the FESEM images. The absorption spectrum suffers intense in lower temperature and tends to shift to lower wavelength in the UV region as the calcination temperature increases. The band gap values were found to be increasing from 3.228-5.550 eV obtained between 500 to 1000 °C, and all the results confirm the formation of willemite phase at 800 °C.

Keywords: Optical properties, Calcination, phosphor, Nanocomposite

1. Introduction

Phosphor host is usually an inorganic material with a large band gap that could be an oxide, silicate, nitride, oxynitride, halide, oxyhalide, selenide or sulfide which is transparent to the incident radiation. Willemite nanoparticles is an interested subject of scientific research and have been studied as an excellent host matrix for dopants such as transition metals ions and rare earth because of high quantum efficiency, super chemical and thermal stability, less expensive and water resistance [1-5]. Willemite as a suitable phosphor material has a tremendous potential application as photonic devices [6], laser crystal [7] and opto-electronics [8].

Various methods and techniques have been employed by researchers to produce pure and doped willemite. Such as solid state reaction [5], sol-gel method [1], chemical vapour method [9], hydrothermal method [10], supercritical water method [11], spray pyrolysis method [12], solvothermal method [13]. However, most of these methods involve difficulty in larger scale production due to the complicated procedure and expensive cost involved, the high reaction temperature, longer time of reaction, toxic chemical reagent and by-product released to the environment which has a potential harm. A simple thermal treatment route was employed to prepare willemite nanoparticles because of its simplicity, low-cost of production and environmentally friendly [14-16]. The novelty of this work reported the fabrication and syntheses of willemite nanoparticles using simple thermal treatment route and the influence of calcination temperature on the structural and optical properties of the nanoparticle for phosphor materials.

2. Experimental

2.1. Materials

Zinc acetate dihydrate [$Zn(CH_3COO)_2\ 2H_2O$] (M_w = 219.49 g/mol) and silicon tetraacetate reagent [$Si(OCOCH_3)_4$] (M_w = 264.26 g/mol) were purchased from sigma Aldrich and used as precursors, Poly(vinyl pyrrolidone) (PVP M_w = 29000 g/mol) was also purchased from sigma Aldrich which served as capping agent, hence reduce agglomeration and stabilize the nanoparticles. Deionized water was used as a solvent. All chemicals used were about 99% purity and was used without further purification.

* MATERIAL SYNTHESIS AND CHARACTERIZATION LABORATORY (MSCL), INSTITUTE OF ADVANCED TECHNOLOGY (ITMA), UNIVERSITI PUTRA MALAYSIA, 43400 UPM SERDANG, SELANGOR, MALAYSIA
** DEPARTMENT OF PHYSICS, FACULTY OF SCIENCE, UNIVERSITI PUTRA MALAYSIA, 43400 UPM SERDANG, SELANGOR MALAYSIA
*** NATIONAL RESEARCH INSTITUTE FOR CHEMICAL TECHNOLOGY ZARIA, KADUNA STATE NIGERIA
**** FMECHANICAL ENGINEERING DEPARTMENTS, FEDERAL POLYTECHNIC, DAMATURU, 620221 YOBE STATE, NIGERIA
***** COVENTRY UNIVERSITY, FACULTY OF ENGINEERING AND COMPUTING, DEPARTMENTS OF MECHANICAL, AUTOMOTIVE AND MANUFACTURING, CV1 5FB, COVENTRY, UNITED KINGDOM

Corresponding authors: khamirul@upm.edu.my; babaiya1@gmail.com

2.2. Methodology

An aqueous solution of PVP was prepared by dissolving 3 g of PVP in 100 ml of deionized water at 70 °C. 0.2 mmol of Zinc acetate dihydrate and 0.1 mmol of silicon tetraacetate was added to the solution and allowed to stir using a magnetic stirrer for 2 hours. The mixed solution was then poured into a clean glass petri dish and the water was evaporated at 80 °C for 24 hours in an oven to dry the sample. The resulting solid obtained was crushed for 20 minutes in a mortar to powder form. The powder was poured into a crucible boats and placed in an electric furnace for calcinations process at the temperatures between 500 and 1000 °C for 3 hours respectively at a heating rate of 2 °C per minutes for the decomposition of the organic compounds and the crystallization of the nanocomposite.

3. Characterization

In this study, several techniques were used to examine the synthesized willemite nanoparticles. The structural behavior of the crystalline sample was analyzed by X-ray diffraction (XRD Shimadzu model 6000 using Cu kα (0.154 nm) as a radiation source to generate diffraction patterns from the sample at an ambient temperature in 2θ within the range of 20-80°. The bond formation of samples has been studied by infrared spectra (FT-IR, Perkin Elmer model 1650). The morphological behavior of the sample was examined using FESEM (JEOL JSM-7600F) equipped with EDX and mean linear intercept method was used for measuring the grain size. The particle size distribution was observed by Transmission electron microscopy (JEOL TEM model 2010F UHR) with an accelerating voltage of 200 kV. The optical properties were determined by UV-vis spectra meter (Shimadzu model UV-3600) at room temperature in the range of 200-800 nm.

4. Results and discussion

4.1. Formation Mechanism of willemite

PVP is a water-soluble and synthetic biodegradable polymer. The zinc acetate dihydrate [$Zn(CH_3COO)_2.2H_2O$] was dissolved in aqueous PVP and deionized water. The metallic ions are entrapped by ionic-dipole interaction with an amine group in the polymeric chains. While silicon tetraacetate reagent [$Si(OCOCH_3)_4$] was added to the solution, precipitations were observed and thus remain as a solid phase in the solution. The water in the sample was eliminated simply by drying and the ions left behind were immobilized in the polymer scaffold. After the application of heat, polymer content and unwanted anions were entirely removed and gradually with continued increase in temperature willemite phase formed.

4.2. TGA-DTG measurements

The right temperature to commence the calcination process was determined by thermogravimetric measurement and its derivative (TGA-DTA). Fig. 1 indicates the weight-loss percentage as a function of the temperature of the dried sample before the calcination. The sample shows two distinct decomposition stages. The initial was weight loss at 84 °C was attributed to the moisture already contained in the sample. The second phase of weight loss was observed at a temperature of 434 °C which indicates that most PVP has been decomposed. There is no significant weight loss the moment the temperature reaches 485 °C; this is due to complete decomposition of PVP thereby turning into a carbonaceous product, such that only the metal oxide remains as final residue [14,17].

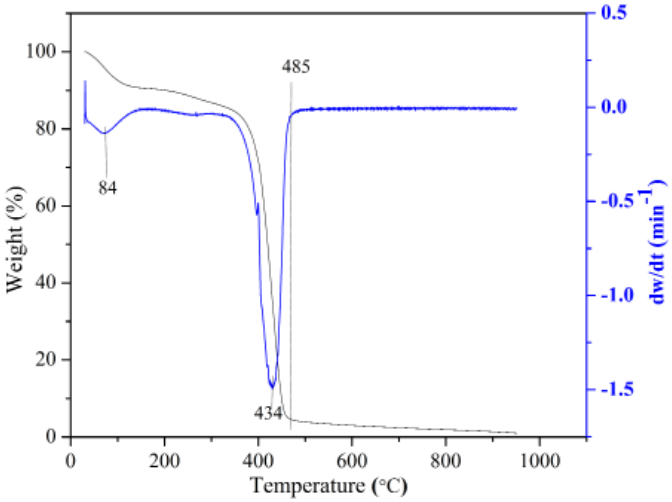

Fig. 1. Thermogravimetric (TG) and thermogravimetric derivative (DTG) curves for PVP at a heating rate of 10 °C/min under N_2 condition

4.3. FT-IR analysis

FT-IR spectroscopy aid in analyzing multi-component and gives the related information of the material phase composition and the nature of interaction existing in various kinds of polymers. In this study, FT-IR is used to determine the organic and inorganic behavior of the sample before and after calcination within the range of 280-400 cm^{-1} as shown by the FT-IR spectra in Fig. 2. The sample before calcination at room temperature reveals the presence of organic sources due to PVP is shown in Fig. 2(a). The vibrational band of N-H, C-H, and C = O stretching vibration were observed at wavenumber 2945, 3414 and 1648 cm^{-1} respectively [14,17]. The peak observed at 1428 cm^{-1} was attributed to C-H bending vibrations originated from methylene group. The band at 1277 cm^{-1} was due to C-N stretching [15], and the two different bands observed at 838 cm^{-1} and 639 cm^{-1} were attributed to C-C ring and C-N = O bending vibration, respectively [17]. While the sample was calcined from 500 to 1000 °C for 3 hours, the broad bands due to the organic material (PVP) has been totally decomposed and disappeared, only vibrational spectra of metal oxide nanoparticles observed.

The vibration band of metal oxide is known to occur at lower wave number below 1000 cm^{-1}. The sample calcined at 500, 600 and 700 °C in Fig. 2(b-d) shows two strong absorption peak in each spectrum at wavenumber 407, 403, 401 and 917, 915 and 912 cm^{-1} which was attributed to Zn-O symmetric stretching vibration and Si-O symmetric stretching vibration respectively [5]. Three strong absorption peaks in each spectrum were also observed while the calcination temperature was increased from 800 to 1000 °C shown in Fig. 2(e-g). The wave number at 380, 377, and 375 cm^{-1} was due to Zn-O symmetric stretching vibration of the sample calcined at 800, 900 and 1000 °C, respectively. Nevertheless, the wave number at 578, 576 and 574 cm^{-1} respectively was due Zn-O asymmetric stretching vibration. The wave number at 885, 887 and 889 cm^{-1} was attributed to Si-O stretching vibration. The slight shift in wave number observed was due to increase in thermal application [18].

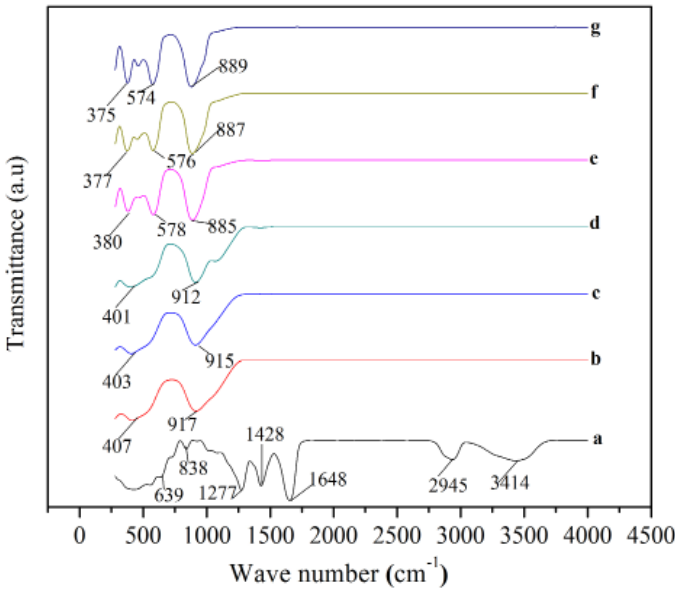

Fig. 2. FT-IR spectra of (a) PVP at 30 °C and ZnO-SiO_2 nanocomposite calcined at (b) 500, (c) 600, (d) 700, (e) 800, (f) 900 and (g) 1000 °C in the range of 280-4500 cm^{-1}

4.4. EDX analysis

The elemental composition of the sample calcined at 1000 °C was investigated by the use of electron disperse X-ray spectroscopy (EDX) as shown in Fig. 3, Zn, Si, and O are present in the sample indicated by their respective peaks which confirmed their presence. The carbon peak detected in the sample was due to the carbon tape used for holding the sample while preparing for the EDX analysis.

4.5. X-ray diffraction analysis

Fig. 4 presents the XRD patterns of the sample before and after the calcination. The observed broad spectrum of the precursor before calcination was due to the amorphous form though it seems to be dried crystal from observation [14]. As the sample was calcined at 500 °C, the spectrum shows sharper diffraction peaks which clearly indicates the crystallinity and the formation of wurtzite structure of ZnO nanoparticles (JCPDS No 01-079-2205) which was unaffected up to 600 °C [19]. The values of the diffraction peaks was positioned at 2θ = 31.67, 34.37, 36.24, 47.47, 56.42, 62.75, 66.27, 67.87, 68.95, 72.02 and 76.96°. These peaks positions tallies with the (010), (002), (011), (012), (110), (013), (020) (112), (021), (004) and (022) diffraction planes of ZnO wurtzite structure. At 700 °C, the XRD spectrum reveals both ZnO and SiO_2 (ICSD No. 170533) phases. The formation of willemite (α-Zn_2SiO_2) phase occurred as the calcination temperature was increased to 800 °C, with all the diffraction peaks indexed to the standard pattern of α-Zn_2SiO_2 (JCPDS No 37-1485), except a trace of unreacted ZnO, which was observed at 2θ = 36.37°. When the temperature is above

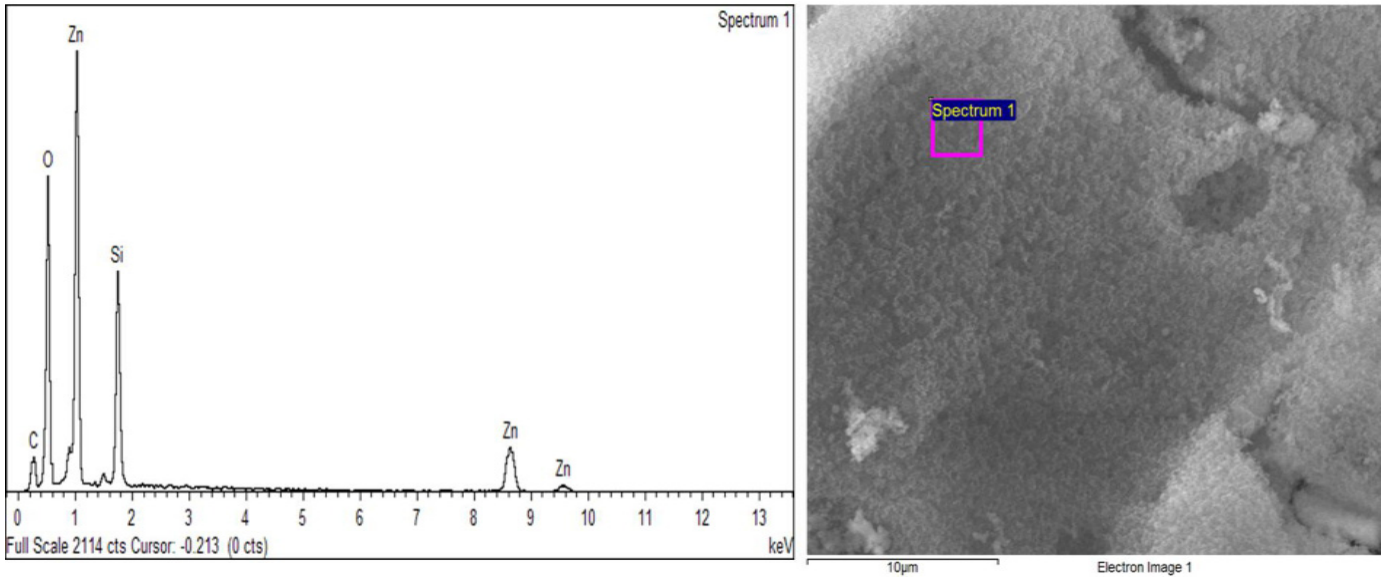

Fig. 3. EDX spectrum of willemite calcined at 1000 °C

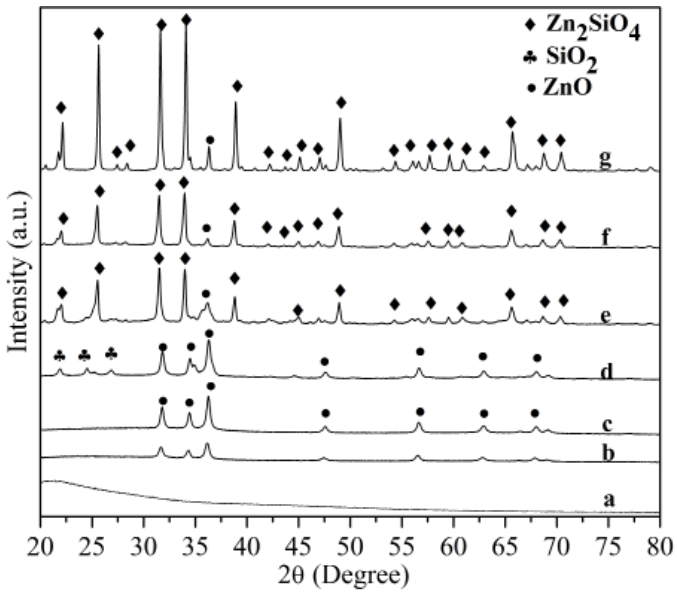

Fig. 4. XRD patterns of ZnO-SiO_2 nanocomposite at different calcination temperature at (a) Room temperature, (b) 500, (c) 600, (d) 700, (e) 800, (f) 900 and (g) 1000°C

700 °C, ZnO was reported to be the dominantly diffusing species in the ZnO/SiO_2 couple [19]. Hence, ZnO atom being at the surface will dominantly diffuse toward the silica matrix thus induces the formation of willemite (Zn_2SiO_4). However, with an increase in temperature, this process of diffusion also increases rapidly. Therefore, the crystallinity of the material progressed with an increase in temperature. Thus, the crystal quality of willemite phase improved more at 900 and 1000 °C. Furthermore, 800 °C which appeared to the phase formation temperature was much lower than the annealing temperature of conventional solid state method and 400 °C lower than the temperature used in the sol-gel method [3]. Phosphor industries have been criticized for its high energy consumption and carbon emission due the high temperature of annealing involved [20,21]. In this regard, a method that involved low preparation temperature like simple thermal treatment method is considered to be favorable in mitigating energy consumption and carbon emission.

Scherer's formular was used to determine the crystallite size of the nanoparticles for the most intense as shown below

$$D = 0.94\lambda/\beta\cos\theta \quad (1)$$

where D is the crystallite size measured in (nm), β is the full width of the diffraction at half of the maximum intensity measured in radians, θ is the Bragg's angle and λ is X-RAY wavelength of CuKα (0.154 nm) [22]. The mean crystallite size was obtained to be 21.7-44.1 nm obtained between the calcination temperatures of 500-1000 °C as shown in Table 1.

4.6. Morphological and particle size examination

The morphology of the material was studied using FESEM. Fig. 5 shows FESEM image, where the nanocomposite clearly exhibits a spherical morphology as calcined at 500-700 °C. Sub-

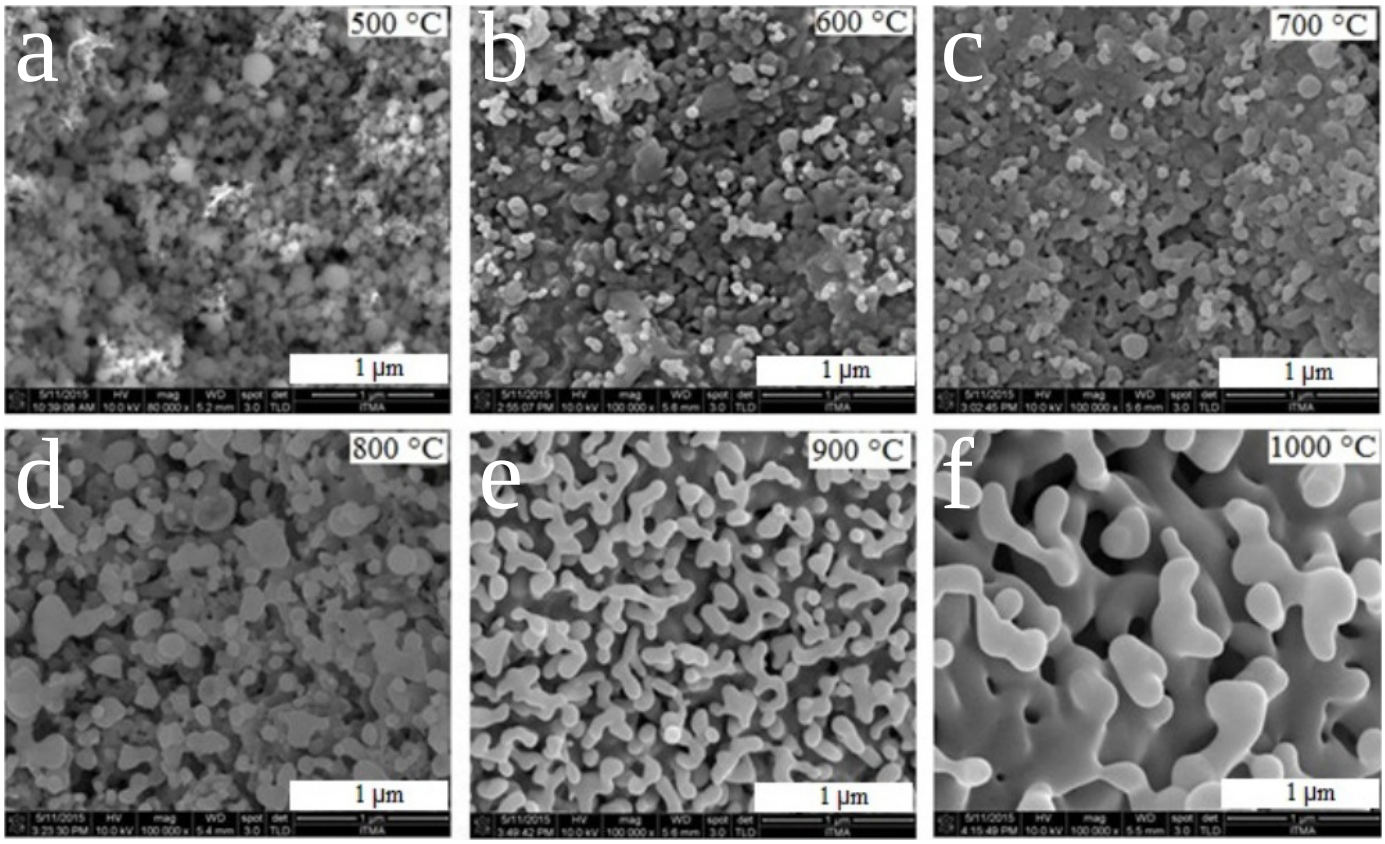

Fig. 5. FESEM images of the ZnO-SiO_2 nanocomposite calcined at various temperature from 500 °C-1000 °C

TABLE 1

Average particle size of $ZnO\text{-}SiO_2$ NPs measured by XRD and comparison of the band gap energy for samples calcined between 500-1000 °C

Temperature (°C)	2θ	FWHM	D_{XRD} (nm)	Lattice Strain %	Eg (eV)
500	36.245	0.389	21.7	0.320	3.228
600	36.282	0.292	29.1	0.389	3.282
700	36.297	0.259	32.8	0.346	3.279
750	—	—	—	—	4.269
800	31.530	0.240	35.1	0.371	5.460
900	33.981	0.227	37.4	0.324	5.527
1000	34.100	0.194	44.1	0.277	5.550

sequently, as the temperature was increased from 800-1000 °C, a dumbbell like structures was formed. These images reveal that the material tends to fuse together to form larger particles at higher calcination temperature [19].

TEM analysis was used to study the particle distribution at different temperatures. Fig. 6 gives the TEM images of the entire sample calcined between 500 to 1000 °C. However, the images obtained shows that the sizes are increasing with the calcination temperature; this has to do with the fact that most of the neighboring particles were fusing together to form larger size particles by melting their surface [23].

4.7. UV-vis analysis

UV-vis absorption spectroscopy was used to study the influence of the calcination temperature on the optical properties. Fig. 7 shows the absorption spectra of nanoparticles at different calcination temperature between 500-1000 °C. The absorption spectrum of 900 and 1000 °C seems to be similar, thus only the spectrum of 900 °C was shown in the Figure for clarity. However, it appears that the intensity of the peak is higher in lower calcination temperature, and it tends to shift to lower wavelength as the annealing temperature increases; this can be attributed to the deterioration of the crystal quality of ZnO [19]. These results clearly imply that willemite (Zn_2SiO_4) phase was formed at 800 °C and the shift to lower wavelength was attributed to the relatively larger band gap (5.460 eV) of willemite.

The influence of the calcination temperature was observed on the optical band gap of the sample as shown in Fig. 8 which was determined from the absorption coefficient value. The energy gap (E_g) is considered in the literature [24] assuming a direct transition between valence and conduction bands given by the expression below.

$$(\alpha hv)^2 = A\,(hv - E_g) \tag{2}$$

Where A is a constant, the photon energy is denoted by hv and E_g is the optical energy band. As shown in Fig. 8 we have plotted the characteristics $(\alpha hv)^2$ versus hv values, where the optical band gap

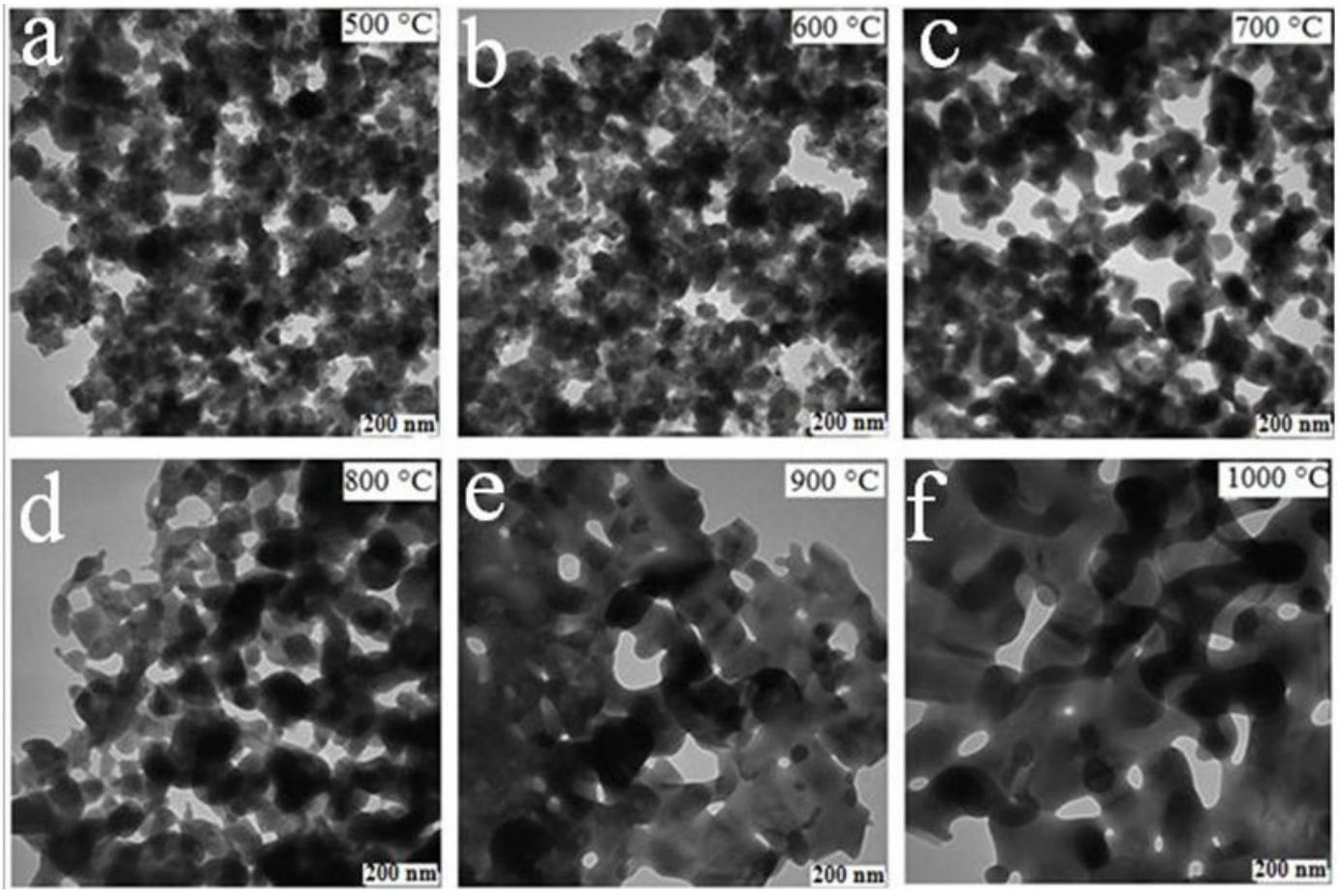

Fig.6. TEM images of the $ZnO\text{-}SiO_2$ nanocomposite at different calcination temperature of (a) 500, (b) 600, (c) 700, (d) 800, (e) 900 and (f) 1000 °C

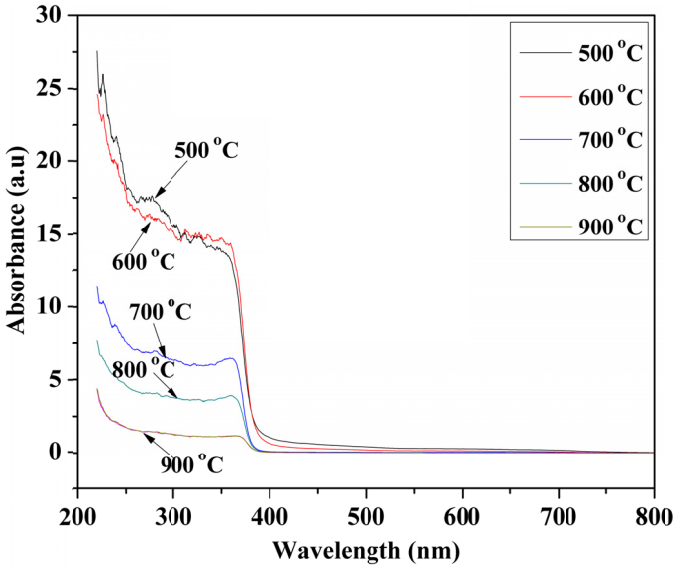

Fig. 7. UV-vis absorption spectra of the ZnO-SiO_2 nanocomposite calcined at various calcination temperatures

of the nanoparticles was determined by simply extrapolating the linear region to where $(\alpha hv)^2$ tends to zero. The optical band gap shown in Fig. 8 and 9 was found to be between 3.228-5.550 eV respectively as the calcination temperature was increase from 500 to 1000 °C. The band gap values obtained were so much

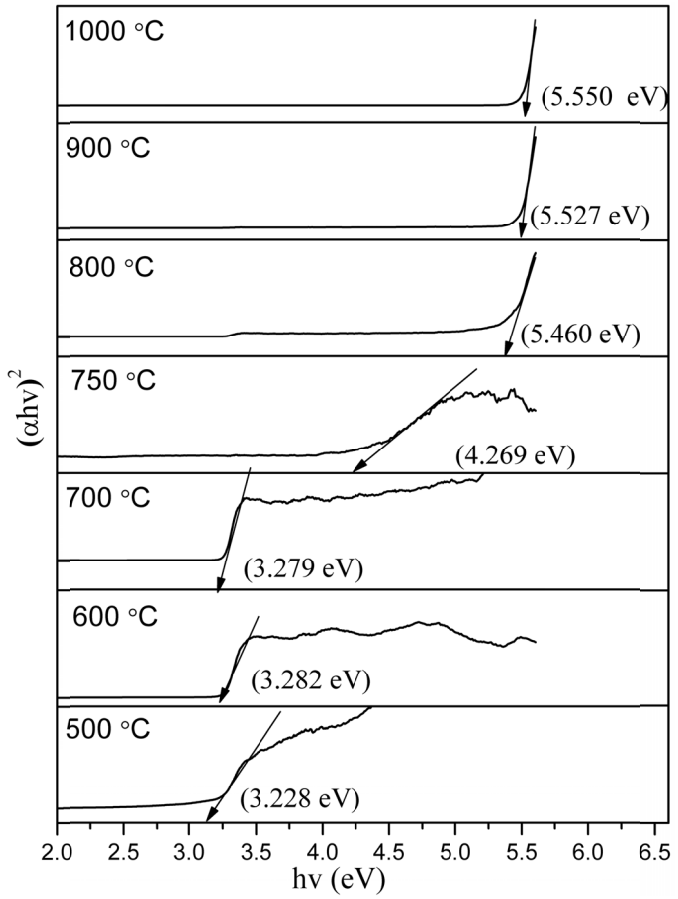

Fig. 8. Optical band gaps of ZnO-SiO_2 nanocomposite calcined at various calcination temperatures

in agreement with the XRD result where the gradual formation willemite phase commenced at 800 °C. Higher calcination above 700 °C is making the ZnO wurtzite structure to collapse in the silica matrix. The nucleation temperature of non-crystalline phase of SiO_2 and crystalline ZnO which allows the formation of willemite was reported to be between 700 °C and 800 °C [25]. This is also evidenced by our XRD result. The optical band gap recorded a significant changes from 3.279 eV at 700 °C to 4.279.5eV when the calcination temperature was elevated to 750 °C, this suggest that the crystal quality of ZnO deteriorates, thus, giving way to the formation of willemite phase at 800 °C with a larger band gap (5.46 eV) [19].

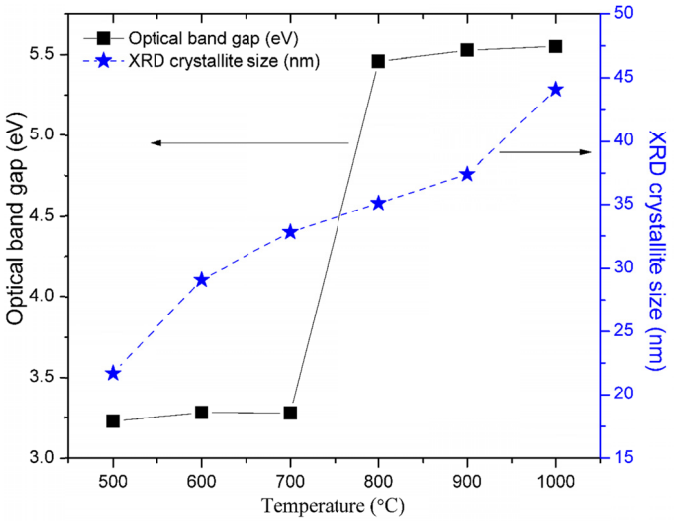

Fig. 9. A graph showing the influence of calcination temperature on the crystallite size and optical band gap of ZnO-SiO_2 nanocomposite

5. Conclusions

Willemite nanoparticles have been successfully synthesized by simple thermal treatment method using only zinc acetate dihydrate [$Zn(CH_3COO)_2$ $2H_2O$] and silicon tetraacetate reagent [$Si(OCOCH_3)_4$] as metal precursors, PVP as a capping agent and deionized water used as a solvent. The heat applied has facilitated the removal of an organic compound and other unwanted ions leaving a residue of crystalline ZnO-SiO_2 nanocomposite. The formation of willemite was obtained at 800 °C, and the crystallinity improved with an increase in calcination temperature, at 900 and 1000 °C as reported in the XRD result. The intensity of the UV-vis absorption peak is higher at a lower temperature, and there was a shift to lower wavelength as the temperature increases. This shift has to do with the fact that the band gap of willemite (Zn_2SiO_4) is higher than ZnO. The band values obtained were in agreement with the XRD result which confirmed the formation of willemite at 800 °C. The simple thermal treatment method is proven to be one of the simplest and low-cost methods to synthesize willemite (Zn_2SiO_4) nanoparticles because it's friendly to the environment due to lack of harmful chemical and toxic by-product effluents.

Acknowledgments

The researchers gratefully acknowledge the financial support for this study from the Malaysian Ministry of Higher Education (MOHE) Grant Number 9531300 and Universiti Putra Malaysia through the International Graduate Research Fund (IGRF) UPM/SPS/GS46148.

REFERENCES

[1] J. El Ghoul, L. El Mir, J. Lumines. **148**, 82-88 (2014).

[2] J. El Ghoul, K. Omri, S.A. Gómez-Lopera, L. El Mir, Opt. Mater. **36**, 1034-1039 (2014).

[3] J. El Ghoul, K. Omri, A. Alyamani, C. Barthou, L. El Mir, J. Lumines. **138**, 218-222 (2013).

[4] J. El Ghoul, L. El Mir, Superlattices Microstruct **82**, 551-558 (2015).

[5] M.H.M. Zaid, K.A. Matori, S.H.A Aziz, H.M. Kamari, Z.A. Wahab, Y.W. Fen, I.M. Alibe, J. Mater. Sci. Mater. El. **27**, 11158-11167 (2016).

[6] S.G., Romanov, A.V. Fokin, R.M. De La Rue, Appl. Phys. Lett.**76**, 1656-1658 (2000).

[7] T.F, Veremeichik, E.V. Zharikov, K.A. Subbotin, Crystallogr. Rep. **48**, 974-988 (2003).

[8] M.H.M. Zaid, K.A. Matori, S.H.A. Aziz, H.M. Kamari, Z.A. Wahab, N. Effendy, I.M Alibe, J. Non. Cryst. Solids. **449**, 107-112. (2016).

[9] A. Roy, S. Polarz, S. Rabe, B. Rellinghaus, H. Zähres, F.E. Kruis, M. Chem. Eur. J. **10**, 1565-1575 (2004).

[10] R. Pozas, V.M. Orera, M. Ocana, J. Eur. Ceram. Soc. **25**, 3165-3172 (2005).

[11] Z.S. Toyama, M. Takesue, T.M. Aida, M. Watanabe, R.L. Smith, J. Supercrit. Fluids **98**, 65-69 (2015).

[12] Y.C. Kang, S.B. Park, Mater. Res. Bull. **35**, 1143-1151 (2000).

[13] S. Takeshita, J. Honda, T. Isobe, T. Sawayama, S. Niikura, Size--tunable solvothermal synthesis of $Zn_2GeO4:Mn^{2+}$ nano phosphor in water/diethylene glycol system, Crystal Growth and Design **10**, 4494-4500 (2010).

[14] I.M. Alibe, K.A. Matori, E. Saion, A.M. Alibe, M.H.M Zaid, E.A.A. Ghapur Engku, Dig. J. Nanomater. Biostruct. **11**, 1155-1164 (2016).

[15] M.G. Naseri, M.H.M. Ara, E.B. Saion, A.H.J. Magn. Magn. Mater. **350**, 141-147 (2014).

[16] M.G. Naseri, H.M. Kamari, A. Dehzangi, A. Kamalianfar, E.B. Saion, J. Magn. Magn. Mater. **389**, 113-119 (2015).

[17] N.M. Al-Hada, E.B. Saion, A.H. Shaari, M.A. Kamarudin, M.H. Flaifel, S.H. Ahmad, S.A. Gene, PloS one **9**, 1-9 (2014).

[18] P.V. Ramakrishna, D. Murthy, D.L. Sastry, K. Samatha, Spectroc. Acta Pt. A-Molec. Biomolec. Spectr. **129**, 274-279 (2014).

[19] K.S. Babu, A.R. Reddy, K.V. Reddy, A N. Mallika, Mater. Sci. Semicond. Process **27**, 643-648 (2014).

[20] J.G, Canadell, M. R, Raupach, Science **320**, 1456-1457 (2008).

[21] X.P, Zhang, X.M, Cheng, Ecological Economics **68**, 2706-2712 (2009).

[22] F. Zhu-Xi, G. Chang-Xin, L. Bi-Xia, L. Gui-hong, Chin. Phys. Lett. **15**, 457 (1998).

[23] Y.Qu, H. Yang, N. Yang, Y. Fan, H. Zhu, G. Zou, Mater. Lett. **60**, 3548-3552 (2006).

[24] N. Kenny, C.R. Kannewurf, D.H. Whitmore, J. Phys. Chem. Solids **27**, 1237-1246 (1966).

[25] B. Babu, S. Buddhudu, J. Spectrosc. Dyn. **4**, 1-5 (2014).